Engineering Science and Technology, an International Journal 18 (2015) 218–228

HOSTED BY

ELSEVIER

Contents lists available at ScienceDirect

Engineering Science and Technology, an International Journal

journal homepage: http://www.elsevier.com/locate/jestch

Full length article

A data-driven adaptive controller for a class of unknown nonlinear discrete-time systems with estimated PPD

Chidentree Treesatayapun*

Department of Robotics and Advanced Manufacturing, CINVESTAV-Saltillo, Ramos Arizpe 25900, Mexico

ARTICLE INFO

Article history:
Received 20 September 2014
Received in revised form
20 December 2014
Accepted 22 December 2014
Available online 29 January 2015

Keywords:
Data-driven control
Fuzzy logic
Discrete-time
Nonlinear systems
DC-motor

ABSTRACT

An adaptive control scheme based on data-driven controller (DDC) is proposed in this article. Unlike several DDC techniques, the proposed controller is constructed by an adaptive fuzzy rule emulated network (FREN) which is able to include human knowledge based on controlled plant's input–output signals within the format of IF-THEN rules. Regarding to this advantage, an on-line estimation of pseudo partial derivative (PPD) and resetting algorithms, which are commonly used by DDC, can be omitted here. Furthermore, a novel adaptive algorithm is introduced to minimize for both tracking error and control effort with stability analysis for the closed-loop system. The experimental system with brushed DC-motor current control is constructed to validate the performance of the proposed control scheme. Comparative results with conventional DDC and radial basis function (RBF) controllers demonstrate that the proposed controller can provide the less tracking error and minimize the control effort.

1. Introduction

Recently, several control algorithms based on data-driven controller (DDC) or model-free adaptive control (MFAC) have been introduced to compensate the requirement of mathematical model developed under the controlled plant for traditional model based control (MBC) schemes [1]. Only the set of input–output data is required to construct those controllers and its stability can be proved under reasonable assumptions [2–4]. Generally, the on-line estimation of pseudo partial derivative (PPD) of the controlled plant is necessary for design DDC schemes [5]. Those estimation techniques can be used under the assumption that PPD varies slowly over the time. The resetting algorithm for PPD is required when the change of control effort is very small. Moreover, many open problems for DCC method are unraveling such as how to verify the generalized Lipschitz condition, how to select the length of PPD vector and how to guarantee the convergence and stability of tracking problems [1].

The stability analysis is barely objective but the optimum controller is usually preferred [6] for several practical control systems. By solving the nonlinear Hamilton–Jacobi–Bellman (HJB), adaptive dynamic programming (ADP) schemes had been developed to minimize an infinite cost function for both the error signal and the control effort [7]. Artificial neural networks (ANN) have been utilized to estimate the nearly optimum solution with value and policy iterations as critic and action networks [8,9]. The inner iteration and the off-line learning phase are required within the sampling interval [10]. The implementation of this control scheme with physical systems is under developing because of the complexity of computation, the requirement of off-line learning phase and the limitation for a class of nonaffine discrete-time systems [11].

In this work, a novel control scheme, which is applied to DC-motor current control application, is proposed without any requirement of mathematical model of the controlled plant. This plant is considered as a class of nonaffine discrete-time systems which can be simplified by the equivalent compact dynamic linearization (CFDL) under reasonable assumptions. The on-line estimation of PPD and resetting algorithm can be neglected by using an adaptive network called fuzzy rule emulated network (FREN) as a direct controller. Furthermore, the completed estimation of plant Jabobian parameter [12] can be omitted because the proposed learning algorithm requires only the approximated minimum and maximum values of PPD. Those minimum and maximum values can be estimated by our technique which will be discussed in

* Tel.: +52 844 438 96 00; fax: +52 844 438 96 10.
E-mail addresses: treesatayapun@gmail.com, chidentree@cinvestav.edu.mx.
Peer review under responsibility of Karabuk University.

http://dx.doi.org/10.1016/j.jestch.2014.12.004

section 4. The relation between armature voltage and current of DC motors can be written in the format of IF-THEN rule as this example "IF *we need to increase armature current* THEN *we must supply more armature voltage*" [13,14]. Those IF-THEN rules can be included to FREN-controller by network's architecture and parameters setting [15,16].

The experimental results with a commercial grade DC-motor validate the control scheme's performance. Moreover, the advantage of the proposed controller is demonstrated by comparative results with the radial basis function (RBF) controller [17] and the conventional DDC scheme [5].

2. DC motor driving and a class of nonlinear discrete-time systems

In Fig. 1, an electronic circuit is designed to drive a brushed DC motor with armature current measurement. In this work, the motor driving system is considered as the nonlinear plant for a class of discrete-time systems which can be described by

$$y(k+1) = f\big(y(k),\cdots,y(k-n_y),u(k),\cdots,u(k-n_u)\big), \tag{1}$$

where $y(k)\in\mathbb{R}$ denotes as the output voltage [V] represented the armature current by U_1 B and R_{3-6} and $u(k)\in\mathbb{R}$ stands for the control voltage [V] at the time index k. The nonlinear function $f(\cdot)$ and system orders n_y and n_u are definitely unknown. This electronic circuit is constructed by a 2-channel operational amplifier U_1 (TL072). Those resistors are given as R_0 10kΩ, R_{1-2} 1kΩ, R_3 10Ω, R_4 1kΩ and R_{5-6} 10kΩ. Two match-pair transistors Q_{1-2} are selected as 2N4921 and 2N4920, respectively. A commercial DC motor model FF-050SK is selected as our demonstration device "M". The current sense circuit has current–voltage gain as

$$y(k+1) = 0.11 I_M, \tag{2}$$

when I_M denotes the motor current [mA]. According to conventional MFAC algorithms, those following assumptions are stated.

Assumption 1: The partial derivatives of $f(\cdot)$ are continuous with respect to the control effort $u(k)$.

Assumption 2: The nonlinear system described in (1) is generalized Lipschitz. That means the positive constant l must be defined when $|\Delta y(k+1)| \le l|\Delta u(k)|$, when $\Delta y(k+1) = y(k+1)-y(k)$ and $\Delta u(k) = u(k)-u(k-1)$.

According to those upper assumptions, the following lemma can be obtained.

Lemma 2.1 *The nonlinear system (1), which is satisfied by assumption 1 and 2 with $|\Delta u(k)|\neq 0$ for time index k, can be transformed into the equivalent compact form dynamic linearization (CFDL) as*

$$\Delta y(k+1) = \Phi(k)\Delta u(k), \tag{3}$$

when $\Phi(k)$ is pseudo partial derivative (PPD), $\Delta y(k+1) = y(k+1)-y(k)$ and $\Delta u(k) = u(k)-u(k-1)$.

The proof of this lemma is given in the appendix A.

In this work, only minimum and maximum boundaries of $\Phi(k)$ are required to design the controller with the following constrain

$$\Phi_m < |\Phi(k)| < \Phi_M, \tag{4}$$

$\forall k = 1,2,\cdots$, when Φ_m and Φ_M stand for minimum and maximum values of $|\Phi(k)|$, respectively. The example and discussion will be given in the section 4 to estimate those values by input–output data set of the controlled plant.

3. Closed-loop system and controller design

The closed-loop control scheme is illustrated by block diagram in Fig. 2. The control effort u forces the output y to follow the desired trajectory r or y_d. This control effort is generated by an adaptive network FREN which can be written as

$$u(k) = \beta^T(k)\phi(e(k)), \tag{5}$$

when $e(k)$ stands for the error signal defined by

$$e(k) = r(k) - y(k). \tag{6}$$

The vector $\beta(k)$ denotes as a set of adjustable parameters and $\phi(k)$ is a vector of membership functions. The setting for both $\beta(k)$ and $\phi(k)$ will be demonstrated later in section 4. To tune adjustable parameters β, the cost function is defined by

$$J(k+1) = \frac{1}{2}\gamma_1 e^2(k+1) + \frac{1}{2}\gamma_2 u^2(k), \tag{7}$$

when γ_1 and γ_2 are positive constants which will be discussed next. Unlike several weight tuning algorithms for neural networks, both tracking error and control effort are able to be minimized. By using a gradient search, the tuning law for β can be obtained as

$$\beta(k+1) = \beta(k) - \eta\frac{\partial J(k+1)}{\partial\beta(k)}, \tag{8}$$

where η denotes as the learning rate. The partial derivative term $\partial J(k+1)/\partial\beta(k)$ can be determined by

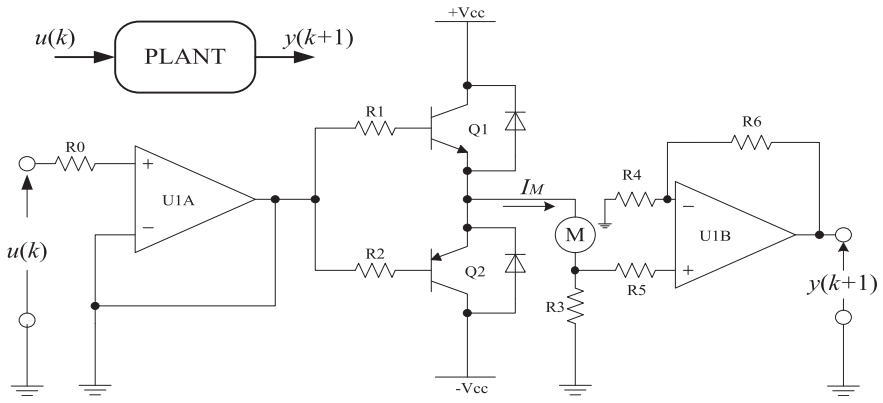

Fig. 1. DC-Motor driving circuit and block diagram.

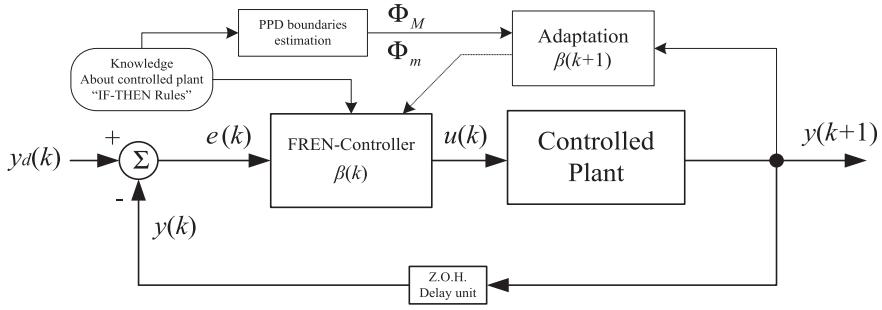

Fig. 2. Control system block diagram.

$$\begin{aligned}\frac{\partial J(k+1)}{\partial\beta(k)} &= \frac{1}{2}\gamma_1\frac{\partial e^2(k+1)}{\partial\beta(k)} + \frac{1}{2}\gamma_2\frac{\partial u^2(k)}{\partial\beta(k)},\\ &= \gamma_1 e(k+1)\frac{\partial e(k+1)}{\partial y(k+1)}\frac{\partial y(k+1)}{\partial u(k)}\frac{\partial u(k)}{\partial\beta(k)} + \gamma_2 u(k)\frac{\partial u(k)}{\partial\beta(k)}\\ &= -\gamma_1 e(k+1)\Phi(k)\phi(k) + \gamma_2 u(k)\phi(k).\end{aligned} \tag{9}$$

Substitute (9) into (8), thus the adaptation law can be obtained as

$$\beta(k+1) = \beta(k) + \eta[\gamma_1 e(k+1)\Phi(k) - \gamma_2 u(k)]\phi(k). \tag{10}$$

The learning rate η in (10) will be considered with constants γ_1 and γ_2. The range of learning rate will be defined to guarantee the convergence and closed-loop performance. According to the dynamic model given by (3), that system can be rearranged as

$$y(k+1) = y(k) + \Phi(k)u(k) - \Phi(k)u(k-1). \tag{11}$$

Substitute (5) into (11), thus the error dynamic can be obtained by

$$e(k+1) = r(k+1) - \Phi(k)\phi^T(k)\beta(k) + \Phi(k)u(k-1) - y(k). \tag{12}$$

Substitute (12) into (10), we have

$$\begin{aligned}\beta(k+1) &= \beta(k) - \eta\left[\gamma_1\Phi^2(k) + \gamma_2\right]\|\phi(k)\|^2\beta(k) + \eta[\gamma_1 r(k+1)\\ &\quad + \Phi(k)u(k-1) - y(k)]\Phi(k)\phi(k),\\ &= \left[I - \eta\left[\gamma_1\Phi^2(k) + \gamma_2\right]\|\phi(k)\|^2\right]\beta(k) + \alpha_\beta(k)\phi(k),\end{aligned} \tag{13}$$

when

$$\alpha_\beta(k) = \eta[\gamma_1 r(k+1) + \Phi(k)u(k-1) - y(k)]\Phi(k). \tag{14}$$

The sequence $\beta(k)$ will be converged when

$$-1 \le 1 - \eta\left[\gamma_1\Phi^2(k) + \gamma_2\right]\|\phi(k)\|^2 \le 1. \tag{15}$$

With positive constants γ_1 and γ_2, it is clear that $[\gamma_1\Phi^2(k) + \gamma_2]\|\phi(k)\|^2 \ge 0$, thus (15) can be rearranged as

$$0 \le \eta \le \frac{2}{[\gamma_1\Phi^2(k) + \gamma_2]\|\phi(k)\|^2}. \tag{16}$$

Regarding to (4), it's clear that

$$0 \le \eta \le \frac{2}{[\gamma_1\Phi_M^2 + \gamma_2]\|\phi(k)\|^2} \le \frac{2}{[\gamma_1\Phi^2(k) + \gamma_2]\|\phi(k)\|^2}. \tag{17}$$

Let's define $0 \le\gamma_\eta \le 2$, thus, the learning rate in (17) can be practically calculated by

$$\eta(k) = \frac{\gamma_\eta}{[\gamma_1\Phi_M^2 + \gamma_2]\|\phi(k)\|^2}, \tag{18}$$

where $\eta(k)$ is time varying learning rate. Regarding to the minimum boundary of $\Phi(k)$ in (4) and a time varying learning rate in (18), the on-line tuning law in (10) can be rewritten as

$$\beta(k+1) = \beta(k) + \eta(k)[\gamma_1 e(k+1)\Phi_m - \gamma_2 u(k)]\phi(k). \tag{19}$$

By using the control scheme proposed in Fig. 2 and the on-line learning algorithm (19), the closed-loop performance will be demonstrated with the following Lyapunov function

$$V(k) = \gamma_v e^2(k) + \gamma_L L(k), \tag{20}$$

when γ_v and γ_L are positive constants which will be discussed later and $L(k)$ is the infinite cost function defined by

$$L(k) = \sum_{l=k}^{\infty}\left[\tau_1 e^2(l) + \tau_2 u^2(l)\right], \tag{21}$$

where τ_1 and τ_2 are positive constants. The change of Lyapunov function can be obtained by

$$\begin{aligned}\Delta V(k) &= V(k+1) - V(k), = \gamma_v\left[[e(k) + \Delta_e(k)]^2 - e^2(k)\right]\\ &\quad + \gamma_L\left[\sum_{l=k+1}^{\infty}\left[\tau_1 e^2(l) + \tau_2 u^2(l)\right] - \sum_{l=k}^{\infty}\left[\tau_1 e^2(l) + \tau_2 u^2(l)\right]\right],\\ &= \gamma_v\Delta_e(k)[\Delta_e(k) + 2e(k)] - \gamma_L\left[\tau_1 e^2(k) + \tau_2 u^2(k)\right],\\ &= \gamma_v\Delta_e^2(k) + 2\gamma_v\Delta_e(k)e(k) - \gamma_L\tau_1 e^2(k) - \gamma_L\tau_2 u^2(k).\end{aligned} \tag{22}$$

when $\Delta_e(k) = e(k+1)-e(k)$ and it can be approximated by

$$\Delta_e(k) \triangleq \frac{\partial e(k+1)}{\partial\beta(k)}\Delta\beta(k). \tag{23}$$

By applying the chain rule, the partial derivative $\partial e(k+1)/\partial\beta(k)$ can be determined by

$$\frac{\partial e(k+1)}{\partial\beta(k)} = \frac{\partial e(k+1)}{\partial y(k+1)}\frac{\partial y(k+1)}{\partial u(k)}\frac{\partial u(k)}{\partial\beta(k)}, = -\Phi(k)\phi(k). \tag{24}$$

Substitute (24) into (23) and use the tuning law (19), thus

$$\Delta_e(k) \triangleq -\Phi(k)\phi(k)\Delta\beta(k), = -\eta(k)\Phi(k)[\gamma_1[e(k)+\Delta_e(k)]\Phi(k) - \gamma_2 u(k)]\|\phi(k)\|^2, = -a_1(k)e(k)+a_2(k)u(k), \quad (25)$$

when $a_1(k)=\eta(k)\gamma_1\Phi^2(k)\|\phi(k)\|^2/1+\eta(k)\gamma_1\Phi^2(k)\|\phi(k)\|^2$ and $a_2(k)=\eta(k)\gamma_2\Phi(k)\|\phi(k)\|^2/1+\eta(k)\gamma_1\Phi^2(k)\|\phi(k)\|^2$. Substitute (25) into (22), thus the change of Lyapunov function can be given by

$$\Delta V(k) = \gamma_v\Delta e^2(k)+2\gamma_v\Delta e(k)e(k), = \gamma_v[-a_1(k)e(k)+a_2(k)u(k)]^2+2\gamma_v[-a_1(k)e(k) + a_2(k)u(k)]e(k), -\gamma_L\tau_1 e^2(k)-\gamma_L\tau_2 u^2(k). \quad (26)$$

By applying Cauchy-Schwarz inequality with (26), we have

$$\Delta V(k) < 2\gamma_v a_1^2(k)e^2(k)+2\gamma_v a_2^2(k)u^2(k)-2\gamma_v a_1(k)e^2(k) + 2\gamma_v a_2(k)u(k)e(k)-\gamma_L\tau_1 e^2(k)-\gamma_L\tau_2 u^2(k), < \left[2\gamma_v a_1^2(k)-2\gamma_v a_1(k)+\frac{1}{2}\gamma_v-\gamma_L\tau_1\right]e^2(k) + \left[4\gamma_v a_2^2(k)-\gamma_L\tau_2\right]u^2(k). \quad (27)$$

The selection of designed constants γ_v, γ_L, τ_1, τ_2, γ_1 and γ_2 will be introduced by the following theorem.

Theorem 1 *For a class of discrete-time nonlinear systems described in (1), let the control effort be generated by (5) and let parameter β be adjusted by (19), then the closed-loop system for the controlled plant, which fulfills CFDL equivalence system in (3) and assumptions 1–2, can be guaranteed as asymptotically stable while*

$$\gamma_v = 2\gamma_L\tau_1, \quad (28)$$

and

$$\frac{\gamma_2}{\gamma_1} < \frac{1}{2}\sqrt{\frac{\tau_2}{2\tau_1}}|\Phi(k)|. \quad (29)$$

The proof of this theorem is addressed in appendix B.

In this work, the ratio γ_2/γ_1 in (29) can be determined without $\Phi(k)$. By using (4), it's clear that $\Phi_m < |\Phi(k)|$, thus (29) is practically determined by

$$\left.\frac{\gamma_2}{\gamma_1}\right|_{\max} = \frac{1}{2}\sqrt{\frac{\tau_2}{2\tau_1}}\Phi_m. \quad (30)$$

With the conclusion, the time varying learning rate $\eta(k)$ is determined by (18) with constants γ_1 and γ_2 to follow the relation given by (30). Thus, the closed-loop performance can be guaranteed under the result of theorem 1. The setting of all designed constants will be demonstrated in the next section by using only input–output data set of the controlled plant.

4. Experimental setup and results

The motor current I_M will be measured by a data acquisition card CONTEC 16-bit AIO-160802L-LPE as the plant's output $y(k+1)$. The control effort $u(k)$ is generated by computer programming based on MATLAB R2008b with DAQ-toolbox 2.13, Windows XP sp3 and Pentium4-3 GHz CPU. Fig. 3 presents the experimental system. The sampling time is given as 1.5 [ms] for each interval for matching the maximum speed of AIO-160802L-LPE and personal computer's performance to implement control algorithms.

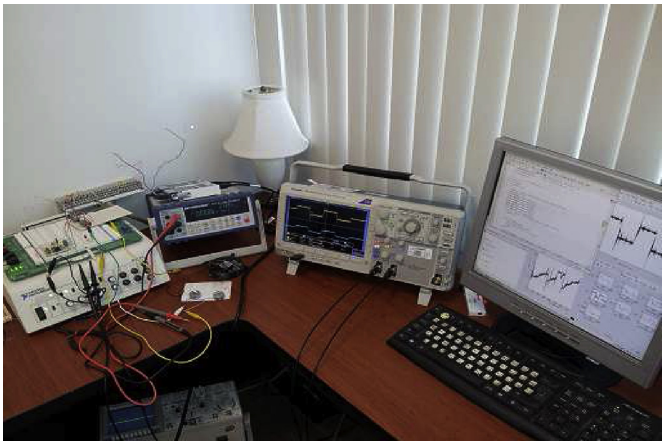

Fig. 3. Experimental setup.

4.1. FREN controller design and results

Let's consider the fact that "IF *we need higher motor current* THEN *we must increase terminal voltage*", thus IF-THEN rules are defined as the followings:

If $e(k)$ is NL	Then $u_1(k)=\beta_{NL}(k)\mu_{NL}(e_k)$,
If $e(k)$ is NM	Then $u_2(k)=\beta_{NM}(k)\mu_{NM}(e_k)$,
If $e(k)$ is NS	Then $u_3(k)=\beta_{NS}(k)\mu_{NS}(e_k)$,
If $e(k)$ is Z	Then $u_4(k)=\beta_{Z}(k)\mu_{Z}(e_k)$,
If $e(k)$ is PS	Then $u_5(k)=\beta_{PS}(k)\mu_{PS}(e_k)$,
If $e(k)$ is PM	Then $u_6(k)=\beta_{PM}(k)\mu_{PM}(e_k)$,
If $e(k)$ is PL	Then $u_7(k)=\beta_{PL}(k)\mu_{PL}(e_k)$,

when N, Z and P denote "negative", "zero" and "positive" linguistic levels respectively, L stands for "large", M is "middle" and S intends for "small".

Fig. 4 illustrates the shape of designed membership functions $\mu(e(k))$ to cover the expected range within $e(k)\in\pm 50$ [mA]. The initial of parameters β can be given by the followings:

Parameter	Value [V]	Parameter	Value [V]
$\beta_{NL}(1)$	−2.5	$\beta_{PS}(1)$	0.75,
$\beta_{NM}(1)$	−1.25	$\beta_{PM}(1)$	1.25,
$\beta_{NS}(1)$	−0.75	$\beta_{PL}(1)$	2.5,
$\beta_{Z}(1)$	0		

The relation of initial setting with membership values is depicted by Fig. 5 to demonstrate the range of motor's terminal voltage. In this application, this range can be given by motor's specification as ±2.5 [V]. Regarding to the control law in (5), those control vectors can be defined as $\beta(k)=[\beta_{NL}(k)\quad \beta_{NM}(k)\cdots\beta_{PL}(k)]^T$ and $\phi(k)=[\mu_{NL}(e_k)\quad \mu_{NM}(e_k)\cdots\mu_{PL}(e_k)]^T$. It's clear that β_{NL} is the largest voltage on the negative side and β_{PL} is the largest voltage on the positive. Those values are designed to cover the motor operating range ±2.5 [V] completely.

To estimate parameters Φ_M and Φ_m, the experimental setup is performed by monitoring motor current with ramp input-voltage 0 to 1.5 [V] and 0 to −1.5 [V]. Fig. 6 shows the result with estimated lines. The ratios between motor current and terminal voltage can be determined by

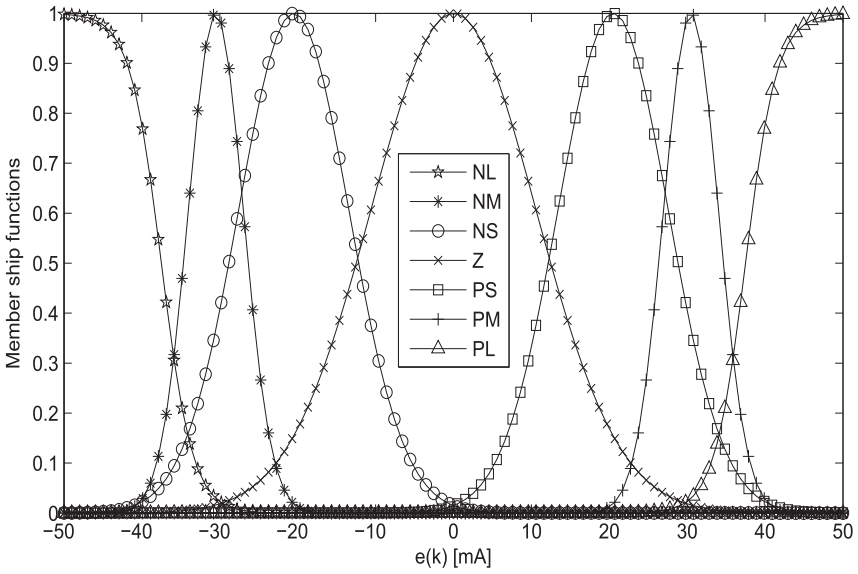

Fig. 4. Membership functions setting.

$$\frac{\Delta I_p}{\Delta V_p} = \frac{19.5 - 0.7}{1.5 - 0.29} = 15.537\left[\frac{\text{mA}}{\text{V}}\right], \tag{31}$$

on the positive side and

$$\frac{\Delta I_n}{\Delta V_n} = \frac{-17.2 + 0.8}{-1.5 + 0.5} = 16.4\left[\frac{\text{mA}}{\text{V}}\right], \tag{32}$$

on the negative side. The constant Φ_M is designed by the calculation results in (31) and (32) while another constant Φ_m is estimated by 10-time reduction from Φ_M. For summary, designed constants are given as the followings:

Constant	Value	Constant	Value
γ_η	0.5	τ_1	1,
γ_1	1	τ_2	1,
γ_2	0.5	γ_L	1,
γ_v	2	Φ_M	20,
		Φ_m	2.

The constant γ_v is determined by (28) and the ratio of γ_2 and γ_1 meets the requirement in (29) to follow the main theorem.

The experimental results of FREN-controller are illustrated in Fig. 7. The signal in channel-1 represents the motor current I_M when the desired motor current y_d is rectangular signal ±30 [mA] or ± 3.3 [V] with current–voltage gain in (2). The control effort u is illustrated in Fig. 7 as V_{in} by channel-2. The time varying of learning rate obtained by (18) is depicted by Fig. 8. Fig. 9 represents the time varying square norm $\|\beta\|^2$ of adjustable parameters.

4.2. Comparative results

To demonstrate the advantage of proposed controller, RBF neural network and data driven control schemes are implemented to our motor driving system.

The basis functions of RBF controller are selected as the same as membership functions for FREN depicted in Fig. 4 and the network architecture is constructed as [18]. The back propagation is integrated to tune weight parameters with convergence and stability proof provided by [17]. The tracking performance and the control effort are illustrated in Fig. 10 with the same designed trajectory as FREN controller. Fig. 11 shows the time varying square norm $\|W\|^2$ of RBF network's weight parameters.

Remark: The initial setting of weight parameters W is same as FREN controller's parameters or $W(1) = \beta(1)$.

Next, the data-driven controller proposed by [5] is applied to drive the motor. This control algorithm can be summarized as follows:

$$u(k) = u(k-1) + \frac{\rho_c \widehat{\phi}(k)}{\lambda + \left|\widehat{\phi}(k)\right|^2}[y_d(k+1) - y(k)], \tag{33}$$

$$\widehat{\phi}(k) = \widehat{\phi}(k-1) + \frac{\eta_c \Delta u(k-1)}{\mu + \Delta u(k-1)^2}\left[\Delta y(k) - \widehat{\phi}(k-1)\Delta u(k-1)\right], \tag{34}$$

when ρ_c and η_c are sequences of step length, λ and μ are weighted factors and $\widehat{\phi}(k)$ is the estimated PPD. The resetting algorithm is required as the following:

$$\widehat{\phi}(k) = \widehat{\phi}(1), \quad \text{if} \quad \left|\widehat{\phi}(k)\right| \le \varepsilon_c \quad \text{or} \quad |\Delta u(k-1)| \le \varepsilon_c, \tag{35}$$

where ε_c is a small positive constant. The tracking performance is shown in Fig. 12 with the same desired trajectory as FREN controller case when channel 1 and 2 represent the motor current by using current–voltage gain in (2) and the control effort, respectively. The online estimation of PPD $\widehat{\phi}(k)$ is illustrated by Fig. 13. In this application, the initial setting of PPD is given by Φ_M or $\widehat{\phi}(1) = \Phi_M = 20$. Generally, the initial setting of PPD can be defined by small positive value. In this work, this initial is given as $\widehat{\phi}(1) = 1$. The responses are shown in Fig. 14 for both tracking performance and control effort. Fig. 15 represents the online estimation $\widehat{\phi}(k)$. The extreme variation of $\widehat{\phi}(k)$ can be observed with this setting.

To summarize, Table 1 demonstrates comparative results by using sum square of total control effort and tracking error. It's clear that the proposed controller can provide less control effort and tracking error. A parameter T_c denotes computation time which is

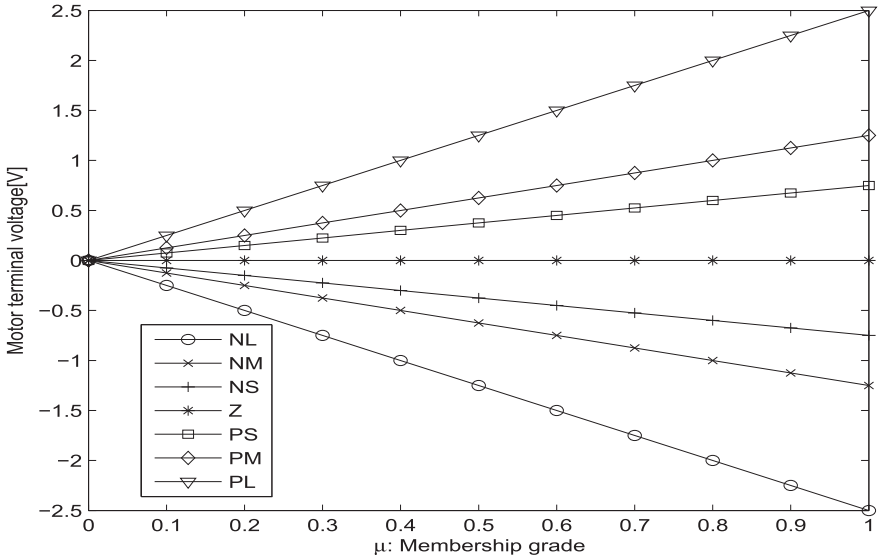

Fig. 5. Initial setting of adjustable parameters $\beta(1)$.

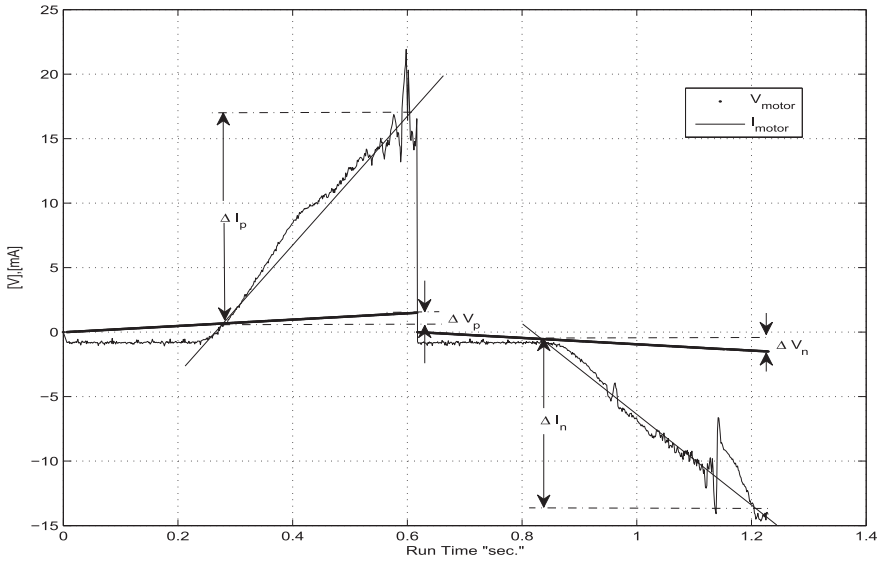

Fig. 6. DC motor: Relation between Voltage and Current.

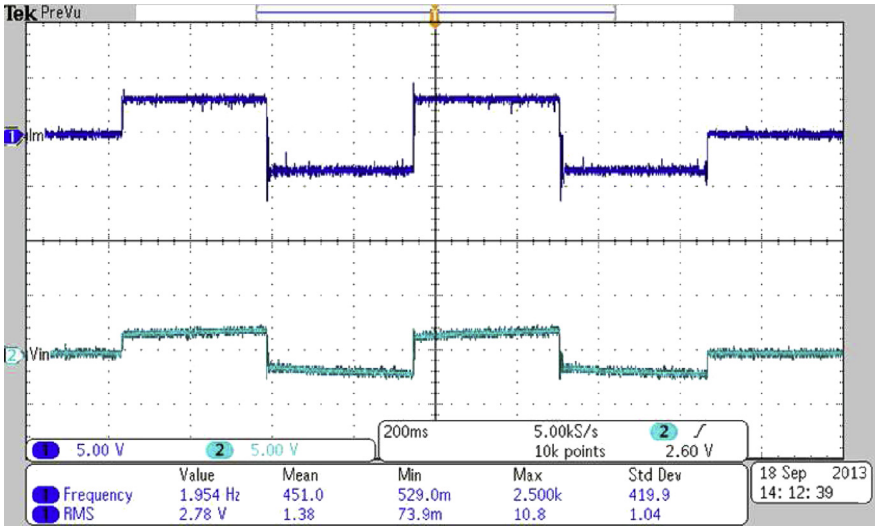

Fig. 7. Motor current and control voltage: FREN controller.

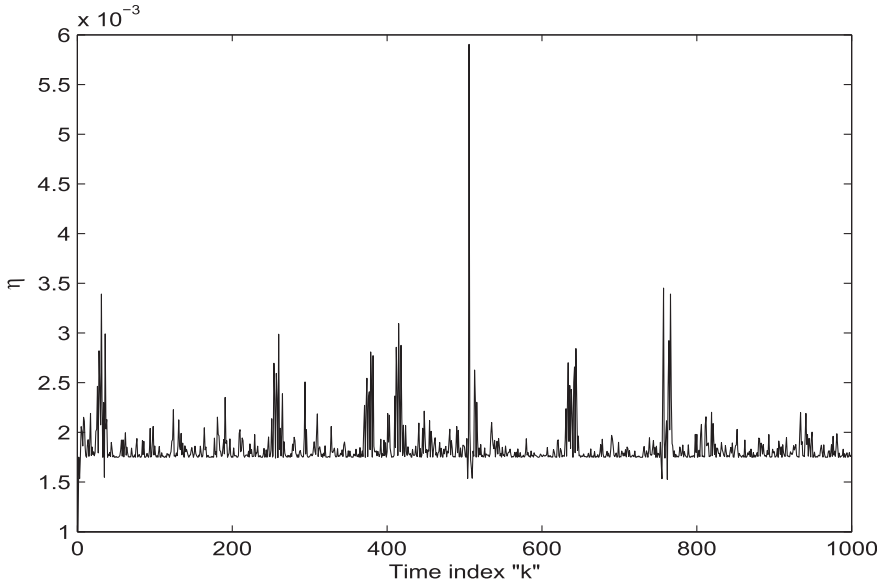

Fig. 8. Time varying learning rate: FREN controller.

used to evaluate the complexity of control schemes. Furthermore, a constant Φ_M obtained from FREN controller can be selected as a good candidate for the initial setting $\widehat{\phi}(1)$ in DDC scheme.

5. Conclusion

A model-free adaptive controller based on FREN has been proposed to control the armature current of commercial DC-motors. This controller is simply designed by the general knowledge of controlled plants. Any mathematical model or system dynamic can be neglected here. In this case, the control plant is a commercial DC-motor with armature current tracking control, thus, the knowledge within IF-THEN rules can be defined as "IF *we need higher motor current* THEN *we must increase terminal voltage*". Moreover, the system analysis has been developed from DDC schemes which allow us to consider the controlled plant as "unknown system". The motor driving plant has been considered as a class of non-affine discrete time system which can be simplified by CFDL as the general application of DDC. In this work, the on-line estimation of PPD and resetting algorithm, which is generally required by common DDC schemes, can be neglected because of FREN's IF-THEN rules created by relation between motor's current and voltage. The proposed controller requires only maximum and minimum values of PPD. Fortunately, those values can be directly estimated by the relation of plant's input–output as the demonstration given in section 4. The cost function has been proposed to minimize for both tracking error and control effort energy. Those control constrains such as the learning rate η, cost function's parameters (γ_1 and γ_2) and so on have been considered for the learning algorithm to tune all adjustable parameters inside FREN.

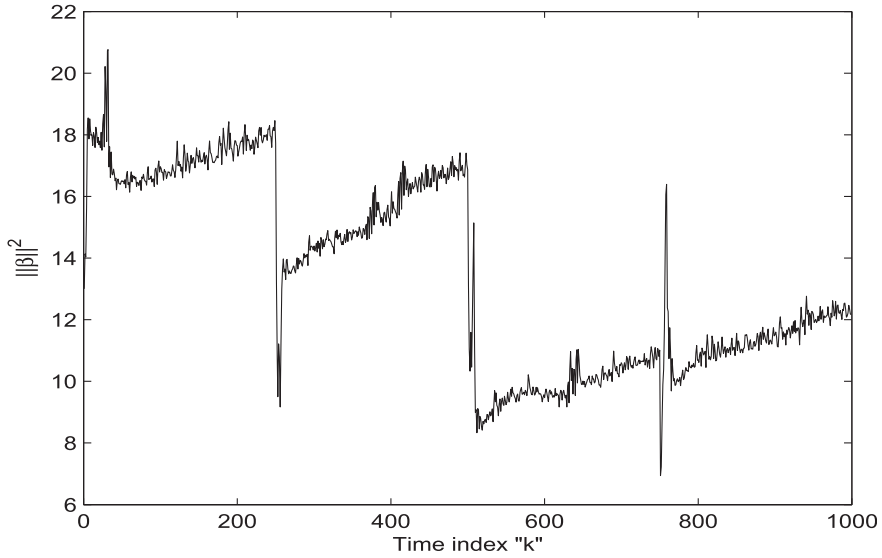

Fig. 9. Time varying of $\|\beta(k)\|^2$: FREN controller.

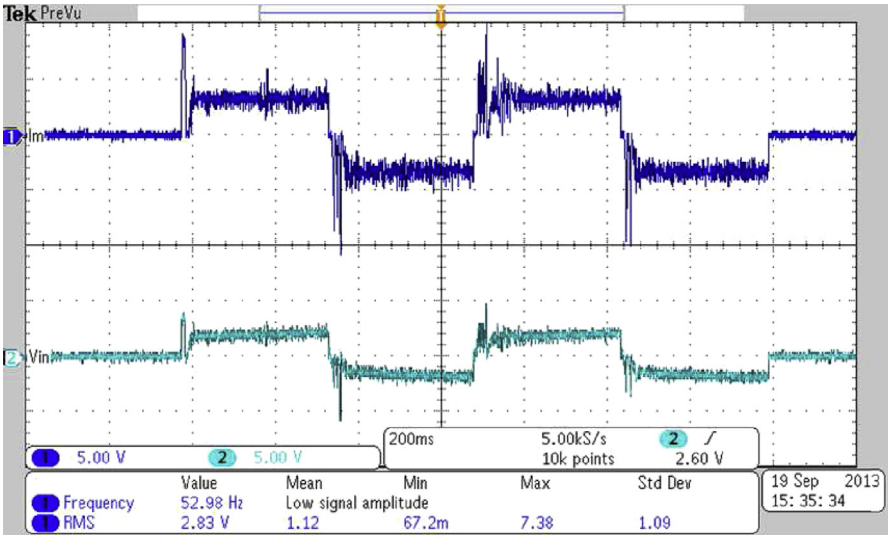

Fig. 10. Motor current and control voltage: RBF controller.

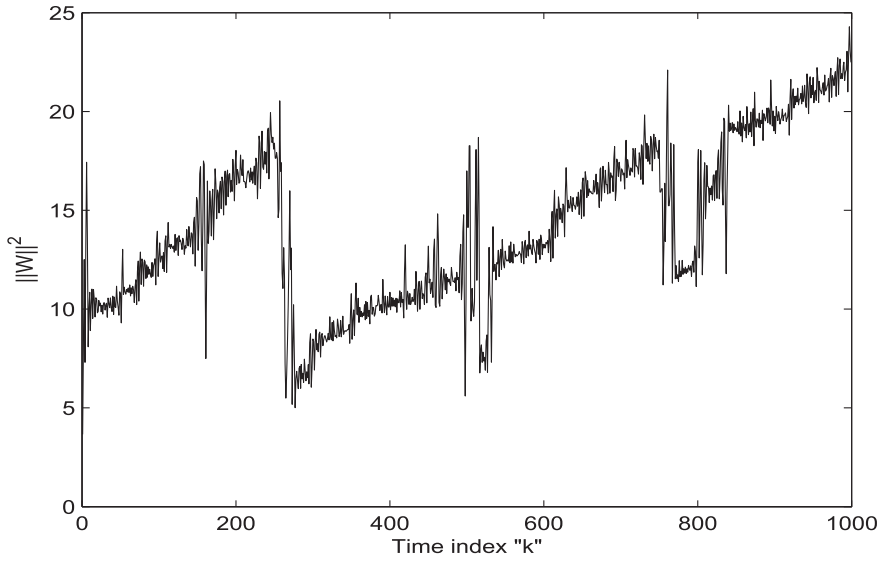

Fig. 11. Time varying of $\|W(k)\|^2$: RBF controller.

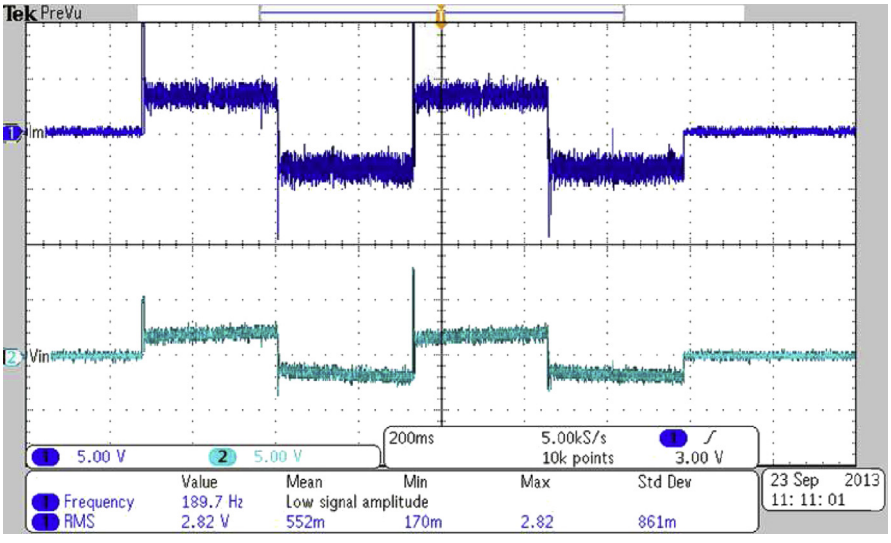

Fig. 12. Motor current and control voltage: Data driven controller $\widehat{\phi}(1) = \Phi_M = 20$.

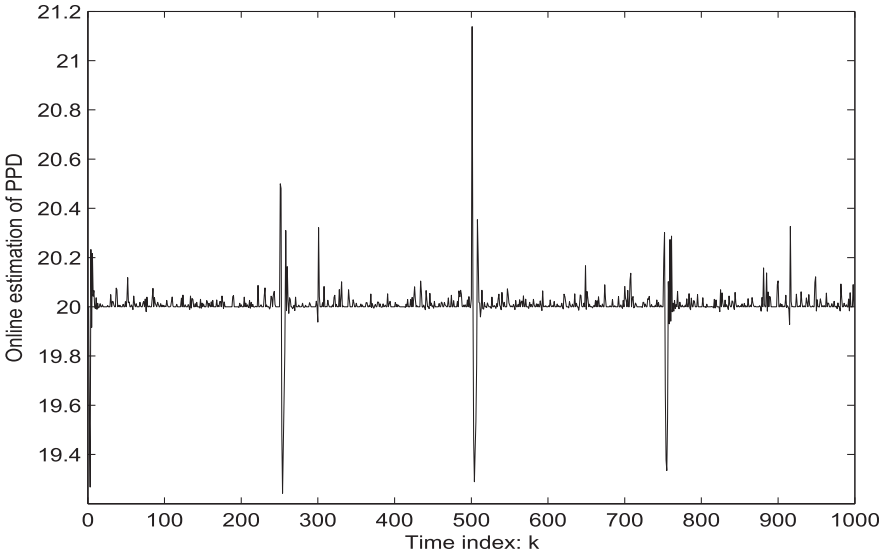

Fig. 13. Time varying of $\widehat{\phi}(k)$: Data driven controller $\widehat{\phi}(1) = \Phi_M = 20$.

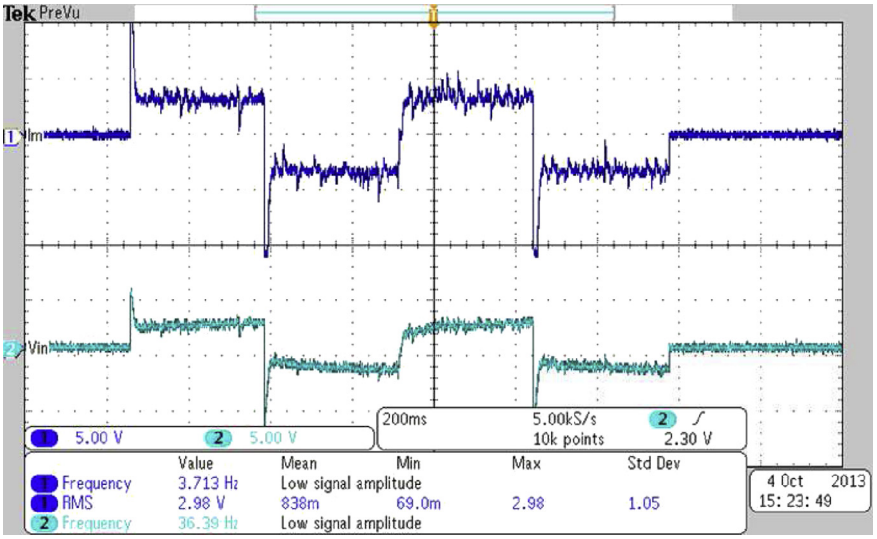

Fig. 14. Motor current and control voltage: Data driven controller $\widehat{\phi}(1) = 1$.

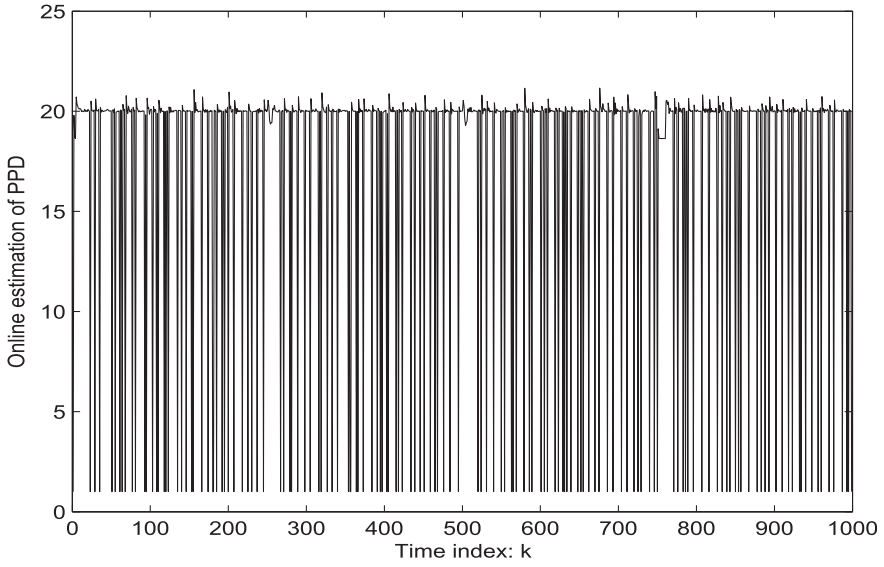

Fig. 15. Time varying of $\widehat{\phi}(k)$: Data driven controller $\widehat{\phi}(1) = 1$.

Table 1
Performance comparison results.

	RBF	DDC $\widehat{\phi}(1)=\Phi_M$	DDC $\widehat{\phi}(1)=1$	FREN
$\sum u^2(k)$	5.548×10^3	3.176×10^3	3.859×10^3	3.001×10^3
$\sum e^2(k)$	1.219×10^6	7.134×10^4	1.051×10^5	3.123×10^4
T_c [ms]	1.4	1.3	1.3	1.4

The closed-loop performance and stability issues have been guaranteed by Lyapunov method with control constrains.

Comparative results with the RBF-controller and the DDC scheme have demonstrated the proposed controller's advantage as the less tracking error and control effort.

A. Proof of Lemma 2.1

Proof:

From the dynamic system given by (1), the change of $y(k+1)$ can be written by

$$\begin{aligned}\Delta y(k+1)&=y(k+1)-y(k),\\&=f\left(y(k),\cdots,y(k-n_y),u(k),\cdots,u(k-n_u)\right)\\&\quad-f\left(y(k-1),\cdots,y(k-n_y-1),u(k-1),\cdots,u(k-n_u-1)\right),\\&=f\left(y(k),\cdots,y(k-n_y),u(k),\cdots,u(k-n_u)\right)\\&\quad-f\left(y(k),\cdots,y(k-n_y),u(k-1),\cdots,u(k-n_u\right),\\&\quad-f\left(y(k-1),\cdots,y(k-n_y-1),u(k-1),\cdots,u(k-n_u-1)\right)\\&\quad+f\left(y(k),\cdots,y(k-n_y),u(k-1),\cdots,u(k-n_u)\right).\end{aligned}\tag{A.1}$$

By using the differential mean value theorem and assumption 1, (A.1) can be rewritten as

$$\begin{aligned}\Delta y(k+1)&=\chi_1\left(y(k),\cdots,y(k-n_y-1),u(k-1),\cdots,u(k-n_u-1)\right)\\&\quad+\frac{\partial f^*}{\partial u(k)}\Delta u(k),\end{aligned}\tag{A.2}$$

when $\chi_1(y(k),\cdots,y(k-n_y-1),u(k-1),\cdots,u(k-n_u-1))=f(y(k),\cdots,y(k-n_y),u(k-1),\cdots,u(k-n_u))-f(y(k-1),\cdots,y(k-n_y-1),u(k-1),\cdots,u(k-n_u-1))$ and $\partial f^*/\partial u(k)$ denotes the partial derivative operation of f with respect to u which is a point within $[u(k),u(k-1)]$. Let repeat the same method, again, we have

$$\begin{aligned}\Delta y(k+1)&=\chi_1\left(y(k),\cdots,y(k-n_y-1),u(k-1),\cdots,u(k-n_u-1)\right)\\&\quad-\chi_1\left(y(k),\cdots,y(k-n_y-1),u(k-2),\cdots,u(k-n_u-1)\right)\\&\quad+\chi_1\left(y(k),\cdots,y(k-n_y-1),u(k-2),\cdots,u(k-n_u-1)\right)\\&\quad+\frac{\partial f^*}{\partial u(k)}\Delta u(k),\\&=\chi_2\left(y(k),\cdots,y(k-n_y-1),u(k-2),\cdots,u(k-n_u-1)\right)\\&\quad+\frac{\partial f^*}{\partial u(k)}\Delta u(k)+\frac{\partial\chi_1^*}{\partial u(k)}\Delta u(k-1).\end{aligned}\tag{A.3}$$

With out any loss on generality, let τ be a control effort length of linearization [5], thus we obtain

$$\begin{aligned}\Delta y(k+1)&=\frac{\partial f^*}{\partial u(k)}\Delta u(k)+\frac{\partial\chi_1^*}{\partial u(k)}\Delta u(k-1)+\cdots\\&\quad+\frac{\partial\chi_\tau^*}{\partial u(k-\tau+1)}\Delta u(k-\tau+1)\\&\quad+\chi_\tau\left(y(k),\cdots,y(k-n_y-1),u(k-\tau),\cdots,u(k-n_u-1)\right).\end{aligned}\tag{A.4}$$

Furthermore, $\chi_\tau(k)$ can be reconsidered as

$$\chi_\tau(k)=\Phi_\chi^T(k)\Delta U(k),\tag{A.5}$$

when $\Delta U(k)=[\Delta u(k),\Delta u(k-1),\cdots,\Delta u(k-\tau)]^T$. On the other hand, we can rewrite (A.4) as

$$\Delta y(k+1)=\vec{\Phi}^T(k)\Delta U(k),\tag{A.6}$$

where

$$\vec{\Phi}(k)=\Phi_\chi(k)+\left[\frac{\partial f^*}{\partial u(k)},\frac{\partial\chi_1^*}{\partial u(k)},\cdots,\frac{\partial\chi_{\tau-1}^*}{\partial u(k)}\right]^T.\tag{A.7}$$

This proof has been done for a general system. When $\tau=1$, the system becomes the CFDL model which can be given be

$$\Delta y(k+1)=\Phi(k)\Delta u(k),\tag{A.8}$$

when $\Phi(k)=\partial f^*/\partial u(k)+\Phi_\chi(k)[:1]$.

B. Proof of theorem 1

Proof:

The change of Lyapunov function obtained in (27) can be negative or $\Delta V(k)<0$ while

$$2\gamma_\nu a_1^2(k)-2\gamma_\nu a_1(k)+\frac{1}{2}\gamma_\nu-\gamma_L\tau_1<0,\tag{B.1}$$

and

$$4\gamma_\nu a_2^2(k)-\gamma_L\tau_2<0.\tag{B.2}$$

Substitute (28) into (B.1), thus we obtain

$$0<\frac{2\gamma_\nu-2\sqrt{2\gamma_\nu\gamma_L\tau_1}}{2\gamma_\nu}<a_1(k)<\frac{2\gamma_\nu+2\sqrt{2\gamma_\nu\gamma_L\tau_1}}{2\gamma_\nu}<1.\tag{B.3}$$

Regarding to $a_1(k)=\eta(k)\gamma_1\Phi^2(k)\|\phi(k)\|^2/1+\eta(k)\gamma_1\Phi^2(k)\|\phi(k)\|^2$, the relation in (B.3) can be rearranged as

$$0<\frac{\eta(k)\gamma_1\Phi^2(k)\|\phi(k)\|^2}{1+\eta(k)\gamma_1\Phi^2(k)\|\phi(k)\|^2}<1,\tag{B.4}$$

while γ_1 is a positive constant thus (B.4) and (B.1) can be held-Substitute $a_2(k)=\eta(k)\gamma_2\Phi(k)\|\phi(k)\|^2/1+\eta(k)\gamma_1\Phi^2(k)\|\phi(k)\|^2$ into (B.2), thus we obtain

$$\frac{\eta(k)\gamma_2|\Phi(k)|\|\phi(k)\|^2}{1+\eta(k)\gamma_1\Phi^2(k)\|\phi(k)\|^2}<\frac{1}{2}\sqrt{\frac{\gamma_L\tau_2}{\gamma_\nu}}.\tag{B.5}$$

By using the fact that $\frac{\eta(k)\gamma_2|\Phi(k)|\|\phi(k)\|^2}{1+\eta(k)\gamma_1\Phi^2(k)\|\phi(k)\|^2}<\frac{\eta(k)\gamma_2|\Phi(k)|\|\phi(k)\|^2}{\eta(k)\gamma_1\Phi^2(k)\|\phi(k)\|^2}$, it leads to

$$\frac{\eta(k)\gamma_2|\Phi(k)|\|\phi(k)\|^2}{\eta(k)\gamma_1\Phi^2(k)\|\phi(k)\|^2}<\frac{1}{2}\sqrt{\frac{\gamma_L\tau_2}{\gamma_\nu}}.\tag{B.6}$$

Substitute (28) into (B.6), thus the ratio of γ_2 and γ_1 can be obtained as

$$\frac{\gamma_2}{\gamma_1} < \frac{1}{2}\sqrt{\frac{\tau_2}{2\tau_1}}|\Phi(k)|. \tag{B.7}$$

It is identical with (29), thus the existence of (B.2) can be guaranteed. Regarding to results within (B.1) and (B.2), the change of Lyapunov function is negative or $\Delta V(k) < 0$, thus the closed-loop system is asymptotically stable.

References

[1] Z.S. Hou, Z. Wang, From model-based control to data-driven control: survey, classification and perspective, Inf. Sci. 235 (2013) 3–35.

[2] D. Meng, Y. Jia, J. Du, F. Yu, Data-driven control for relative degree systems via iterative learning, IEEE Trans. Neural Netw. 22 (12) (Dec. 2011) 2213–2225.

[3] L.D.S. Coelho, W.P. Marcelo, R.S. Rodrigo, A.A.R. Coelho, Model-free adaptive control design using evolutionary-neural compensator, Expert Syst. Appl. 37 (1) (2010) 499–508.

[4] B. Hahn, K.R. Oldham, A model-free ON-OFF iterative adaptive controller based on stochastic approximation, IEEE Trans. Control Syst. Technol. 20 (1) (Jan. 2012) 196–204.

[5] Z.S. Hou, S.T. Jin, A novel data-driven control approach for a class of discrete-time nonlinear systems, IEEE Trans. Control Syst. Technol. 19 (6) (Nov. 2011) 1549–1558.

[6] S.G. Khan, G. Herrmann, F.L. Lewis, T. Pipe, C. Melhuish, Reinforcement learning and optimal adaptive control: an overview and implementation examples, Annu. Rev. Control 36 (2012) 42–59.

[7] A. Al-Tamimi, F.L. Lewis, M. Abu-Khalaf, Discrete-time nonlinear HJB solution using approximate dynamic programming: convergence proof, IEEE Trans. Syst. Man. Cybern. B 38 (4) (Aug. 2008) 943–949.

[8] D. Liu, Q. Wei, Finite-approximation-error-based optimal control approach for discrete-time nonlinear systems, IEEE Trans. Cybern. 43 (2) (Apr. 2013) 779–789.

[9] H. Zhang, Q. Wei, D. Liu, An iterative adaptive dynamic programming method for solving a class of nonlinear zero-sum differential games, Automatica 47 (1) (Jan. 2011) 207–214.

[10] H. Li, D. Liu, Optimal control for discrete-time affine non-linear systems using general value iteration, IET Control Theory Appl 6 (18) (2012) 2725–2736.

[11] T. Dierks, S. Jagannathan, Online optimal control of affine nonlinear discrete-time systems with unknown internal dynamics by using time-based policy update, IEEE Trans. Neural Netw. 23 (7) (Jul. 2012) 1118–1129.

[12] D. Wang, P. Bao, Enhancing the estimation of plant Jacobian for adaptive neural inverse control, Neurocomputing 34 (1–4) (2000) 99–115.

[13] G. Murtaza, A.I. Bhatti, Control of dc motors using sliding mode, in: 9th International Bhurban Conference on Applied Sciences & Technology (IBCAST), Islamabad, Pakistan, Jan. 2012, pp. 37–42.

[14] Y. Son, D. Choi, S. Lim, K. Kim, Robust current control for speed sensorless DC motor drive using reduced-order extended observer, Electron. Lett. 48 (18) (Aug. 2012).

[15] C. Treesatayapun, S. Uatrongjit, Adaptive controller with Fuzzy rules emulated structure and its applications, Eng. Appl. Artif. Intell. 18 (2005) 603–615. Elsevier.

[16] C. Treesatayapun, A discrete-time stable controller for an omni-directional mobile robot based on an approximated model, Control Eng. Pract. 19 (2011) 194–230. Elsevier.

[17] H.G. Han, J.F. Qiao, Adaptive computation algorithm for RBF neural network, IEEE Trans. Neural Netw. 23 (2) (Feb. 2012) 342–347.

[18] Y. Xiaofang, W. Yaonan, S. Wei, W. Lianghong, RBF networks-based adaptive inverse model control system for electronic Throttle, IEEE Trans. Control Syst. Technol. 18 (3) (May. 2010) 750–756.